Journal of Experimental Marine Biology and Ecology 428 (2012) 5–15

Contents lists available at SciVerse ScienceDirect

Journal of Experimental Marine Biology and Ecology

journal homepage: www.elsevier.com/locate/jembe

Mesoscale distribution of protozooplankton communities and their herbivory in the western Scotia Sea of the Southern Ocean during the austral spring

Eun Jin Yang [a,*], Jung-Ho Hyun [b], Dongseon Kim [c], Jisoo Park [a], Sung-Ho Kang [a], Hyoung Chul Shin [a], SangHoon Lee [a]

[a] Korea Polar Research Institute, Get-peal Tower, Yeonsu-Gu, Incheon 406-840, South Korea
[b] Department of Environmental Marine Sciences, Hanyang University, 1271 Sa-1 dong, Ansan, Gyeonggi-do 426-791, South Korea
[c] Korea Ocean Research & Development Institute, 1270 Sa-dong, Ansan, Gyeonggi-do 426-170, South Korea

ARTICLE INFO

Article history:
Received 17 October 2011
Received in revised form 18 May 2012
Accepted 19 May 2012
Avilable online 20 June 2012

Keywords:
Antarctic
Dilution method
Grazing rate
Protozooplankton
Western Scotia Sea

ABSTRACT

The distribution and structure of protozooplankton communities and the impact of their grazing on phytoplankton during spring were studied as part of the 15th Korean Antarctic Research Program in the western Scotia Sea. Water mass identities were determined based on physicochemical properties, with four regions identified: north of the Polar Front (NPF), Polar Front (PF), South of the Polar Front (SPF), and the South Antarctic Circumpolar Current region (SACCr). Physicochemical characteristics of the water column significantly influenced the distribution and structure of phytoplankton and protozooplankton communities. The NPF was characterized by relatively warmer water, low nutrient, low chlorophyll *a* (chl*a*), and pico-sized phytoplankton predominance (i.e., cyanobacteria and eukaryotic picoflagellates). Nano-sized phytoplankton such as *Phaeocystis antarctica* and *Cryptomonas* sp. dominated in the SACCr with its colder water, higher nutrient, and higher chl*a* concentrations. Despite the relatively slightly high chl*a* concentration in the PF, micro-sized phytoplankton, especially diatoms, were abundant. Large changes in protozooplankton biomass and community were observed between water masses. Heterotrophic nanoflagellates including choanoflagellates and nanociliates declined in abundance from the NPF to SACCr, whereas heterotrophic dinoflagellates (HDF) and microciliates increased in abundance from the NPF to SACCr. Ciliates declined in importance from the NPF to SACCr, accounting for over 50% of the total protozooplankton biomass in the NPF. In contrast, HDF comprised over 50% of the total in the SPF, PF, and SACCr. The depth-integrated protozooplankton biomass ranged from 443.2 to 934.0 mg C m^{-2}, and was highest in the PF and lowest in the NPF. These relationships suggest that the spatial variation in the community and biomass of protozooplankton appears to be primarily governed by the community and size structure of phytoplankton. Protozooplankton consumed an average of 76.9% of daily phytoplankton production. Therefore, protozooplankton were the major consumers of the diverse phytoplankton community, and protozooplankton grazing is one of the most important loss processes affecting phytoplankton biomass and composition during spring in the western Scotia Sea.

1. Introduction

The Scotia Sea, which constitutes part of the southwest Atlantic sector of the Southern Ocean, is one of the most productive areas in the Southern Ocean (Brandon et al., 2004; Murphy et al., 2007). Regional circulation in the Scotia Sea is dominated by the eastward flow of the topographically steered Antarctic Circumpolar Current (ACC) (Moore et al., 1997; Orsi et al., 1995; Rintoul and Sokolov, 2001). The ACC is closely associated with three deep-reaching oceanic frontal systems, from north to south: the Subantarctic Front (SAF), the Polar Front (PF), and the Southern ACC Front (SACCF). The southern boundary of the ACC (SB), farther south, separates ACC water from subpolar water (Nowlin et al., 1977; Orsi et al., 1995). This hydrographic diversity, coupled with extreme seasonality, results in dramatic spatial and temporal variability in planktonic community structure (Brown and Landry, 2001; Ward et al., 2006). Primary productivity within the ACC is highly variable, despite the high nutrient–low chlorophyll (HNLC) conditions that persist over much of its extent (Tréguer and Jacques, 1992). In addition, production within the front area is often elevated compared to surrounding oceanic areas, and this elevated production can be spatially extensive (Holm-Hansen et al., 2004; Moore and Abbott, 2002; Ward et al., 2002).

In the pelagic carbon cycle, the role of microbial food webs may vary with trophic conditions and plankton community structure (Wylie and Currie, 1991). The microbial food web has been shown to dominate the food web structure in HNLC systems, such as the Southern Ocean and the tropical Equatorial Pacific, where small phytoplankton are dominant (Brown et al., 2003; Hall et al., 2004; Safi et

* Corresponding author. Tel.: +82 32 260 6184; fax: +82 32 260 6109.
E-mail address: ejyang@kopri.re.kr (E.J. Yang).

0022-0981/$ – see front matter.
doi:10.1016/j.jembe.2012.05.018

al., 2007). In systems where the microbial food web is dominant, most biogenic material is rapidly recycled within the euphotic layer (Fortier et al., 1994), and protozooplankton play a pivotal role in the transference of carbon from the microbial food web to higher trophic levels. Studies of protozooplankton in the Southern Ocean have emphasized the importance of protozooplankton in microbial communities and their role as major consumers of phytoplankton (Becquevort et al., 2000; Burkill et al., 1995; Froneman and Perissinotto, 1996; Garrison, 1991; Garrison and Buck, 1989; Landry et al., 2001; Pearce et al., 2011; Safi et al., 2007; Selph et al., 2001). However, other studies have reported low levels of grazing by microzooplankton on phytoplankton at times in parts of the Southern Ocean (Caron et al., 2000; Froneman, 2004). Overall, previous research has suggested that knowledge of the structure of the microbial community and protozoan grazing impact, is central to developing an understanding of carbon flux in the Southern Ocean. In the different water conditions of the Southern Ocean, however, comprehensive studies on protozooplankton assemblages have been generally limited to the Weddell Sea, Bellingshausen Sea, and the Atlantic and Indian sectors of the Southern Ocean, particularly the marginal ice-edge zone (Froneman, 2004; Garrison, 1991; Klass, 1997; Safi et al., 2007). Although large-scale oceanographic surveys have been conducted in the Scotia Sea, ecological studies of plankton have concentrated on phytoplankton, mesozooplankton, and krill (Holm-Hansen et al., 2004; Kawaguchi et al., 2004; Korb et al., 2005; Ward et al., 2004). Therefore, this paper represents the first undertaking toward improving our understanding of the phytoplankton–protozooplankton trophic link in the pelagic ecosystem of the western Scotia Sea.

We investigated the mesoscale variations and structure of protozooplankton communities and the impact of their grazing on phytoplankton in different water conditions during the austral spring. In this study, we also discuss the relative significance of protozooplankton community composition in different water columns, and trophic links between the community structures of protozooplankton and phytoplankton.

2. Materials and methods

2.1. Study area

The 15th Korean Antarctic Research Program (KARP) organized a research expedition in the western Scotia Sea of the Southern Ocean from 26 November to 6 December 2001. The study area was situated within the western South Atlantic sector of the ACC, which is located from 53°S to 60°S along 52°W, and crossed by two fronts: the PF and the southern ACC Front.

For the purpose of comparison, the study area was subdivided into four zonal bands, based on the hydrographic characteristics of the regions (Fig. 1; Meredith et al., 2003; Moore et al., 1997; Orsi et al., 1995). These regions were defined as follows: (1) waters north of the PF (NPF, 52–56°S), (2) waters within the PF (PF, 56.2°S), (3) waters south of the PF (SPF, 56.4–58.0°S), and (4) the southern ACC region (SACCr, 59–60.9°S), which includes the southern part of the SACCF and SB.

2.2. Physicochemical parameters

Water temperature was measured *in situ* and instantaneously using a conductivity, temperature, and depth (CTD) meter (SBE 911 Plus, Seabird Electronics Co.). To analyze nutrients, a Niskin rosette sampler was used to take water samples from depths of 3, 10, 20, 30, 50, 75, 100, and 150 m. Water samples for nutrient analysis were filtered through glass filter paper (25 mm; Whatman, Middlesex, UK), placed in acid-cleaned polyethylene bottles, and poisoned with $HgCl_2$ (Kattner, 1999). Nitrate + nitrite (hereafter referred to as nitrate) and silicate concentrations were measured using a flow-injection autoanalyzer (QuikChem AE, Lachat, Loveland, CO, USA) and standard colorimetric procedures (Strickland and Parsons, 1972), and calibrated using brine standard solutions (CSK Standard Solutions, Wako Pure Chemical Industries, Osaka, Japan).

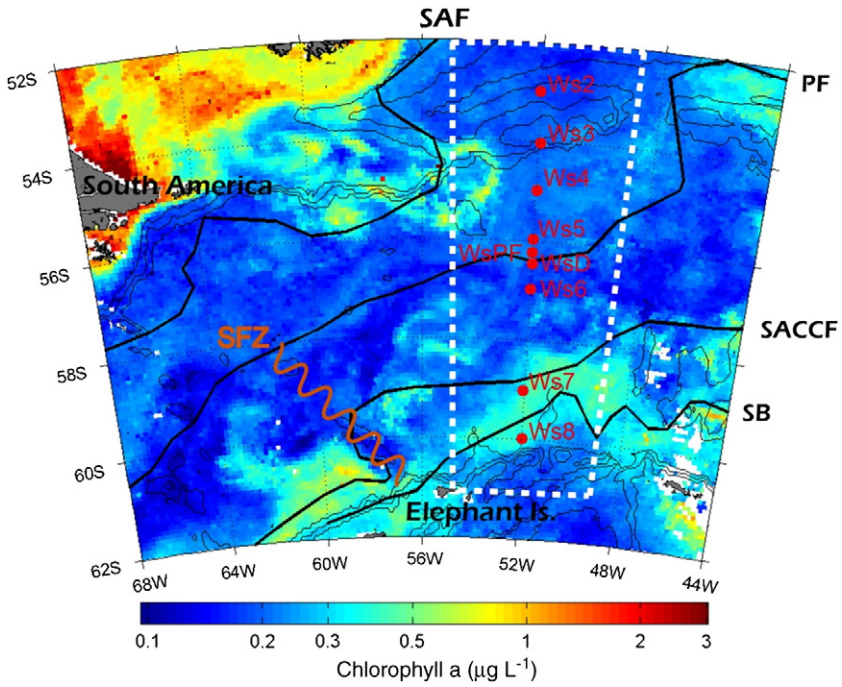

Fig. 1. Stations and monthly composite chlorophyll *a* image (SeaWiFS level 3 data) of the western Scotia Sea on December, 2001. Black lines indicate 1000-, 2000-, and 3000-m isobaths. Four thick lines represent the approximate locations of the sub-Antarctic Front (SAF), Polar Front (PF), Southern Antarctic Circumpolar Current Front (SACCF), and southern boundary of the ACC (SB) (after Orsi et al., 1995; Moore et al., 1997; see also Meredith et al., 2003). SFZ indicates Shackleton Fracture Zone. The rectangle outlined by white dotted lines is the area where chlorophyll *a* was extracted for Fig. 4A.

2.3. Chlorophyll a concentration

Water samples (500 mL) for the determination of total chlorophyll *a* (chl*a*) were taken from each depth and immediately filtered through glass fiber filter paper (25 mm; Gelman). Size-fractionated chl*a* was determined on samples passed sequentially through 20 and 3 μm polycarbonate membrane filters (47 mm) and glass fiber filters (47 mm). The three chl*a* size fractions obtained were referred to as micro-fraction chl*a* (>20 μm), nano-fraction chl*a* (3–20 μm), and pico-fraction chl*a* (<3 μm). Although picoplankton has been defined as being between 0.2 and 2 μm (Sieburth et al., 1978), here we defined picophytoplankton as <3 μm. All filtrations were performed under low vacuum pressure (<100 mm Hg) or by gravity (when using 20-μm mesh and 3-μm filter paper). Size-fractionated chl*a* concentrations were determined by a Turner Design fluorometer (TD-700) using 90% acetone extraction (Parson et al., 1984). The fluorometer was previously calibrated against pure chl*a* (Sigma).

2.4. Protozooplankton and phytoplankton communities

To determine the abundance of protozooplankton, a Niskin rosette sampler was used to take water samples from depths of 3, 10, 20, 30, 50, 75, 100, and 150 m. Water samples for phytoplankton analysis were taken from 10 m, the depth at which dilution experiments were conducted at each station. To determine the abundance of nanoplankton (<20 μm) and microplankton (>20 μm) except ciliates and diatoms, 500-mL samples of water were preserved with glutaraldehyde (1% final concentration) and stored at 4 °C before staining and filtration. Subsamples of 100 mL for nanoplankton and 300 mL for microplankton analysis were filtered onto black 0.8 μm and 8 μm nucleopore filters, respectively, and stained with proflavin (0.33%) and 4′-6-diamidino-2-phenylindole (DAPI; 50 μg mL^{-1} final concentration). At least 50 fields per sample were examined under an epifluorescence microscope (Nikon type 104) at magnifications of 300×–1000×. Autotrophic organisms were distinguished from heterotrophs by the presence of chlorophyll, visualized as red fluorescence under blue light illumination. Most *Phaeocystis antarctica* cells are present as a solitary form in the water column. Solitary *P. antarctica* cells were distinguished from other autotrophic flagellates based on cell size and shape, chloroplast arrangement, and the presence of flagella. For ciliates and diatoms, 500 mL samples of water were preserved with 4% acid Lugol's iodine solution; these were then stored in darkness. Preserved samples were allowed to settle in the mass cylinder for at least 48 h. The upper water was then siphoned out, leaving 50 mL. Next, 5 to 20 mL of each sample were settled in sedimentation chambers before enumeration using an inverted microscope (Olympus IX 70). Samples were counted within 2 months of the sampling date. To estimate the carbon biomass of protozooplankton, the cell volume was calculated by measuring cell dimensions with an ocular micrometer in the microscope (Edler, 1979). Protozooplankton assemblages were classified as heterotrophic nanoflagellates (HNF), choanoflagellates (CNF), ciliates, or heterotrophic dinoflagellates (HDF). The following conversion factors and equations were used to translate cell volume into carbon biomass: 0.19 μg C μm^{-3} for naked ciliates (Putt and Stoecker, 1989); carbon (pg) = 44.5 + 0.053 lorica volume (μm^3) for loricate ciliates (Verity and Langdon, 1984); carbon (pg) = 0.216 × [volume, μm^3]$^{0.939}$ for HDF and CNF (Menden-Deuer and Lessard, 2000); and 220 fg C μm^{-3} for HNF (Bøsheim and Bratbak, 1987).

2.5. Grazing experiments

Phytoplankton growth and protozooplankton grazing rates were determined by the dilution method, measuring the change in total chl*a* concentration during a 24-h incubation (Landry and Hassett, 1982). All equipment for the grazing experiments was cleaned with 10% HCl-Milli-Q water and rinsed thoroughly three times with Milli-Q water before the experiment. Plastic gloves were worn during all phases of the experiment. Water for grazing experiments was collected from within the surface mixed layer at 10-m depth. At each station, 30-L samples of seawater were collected in a Niskin bottle and transferred to a polycarbonate carboy. Filtered water was prepared with gravity filtration from a water bottle through an in-line filter capsule (Gelman Critcap 100, 0.2-μm pore size, pre-washed with 10% trace-metal grade HCl followed by Milli-Q and seawater rinses) to clean the polycarbonate bottle. The experimental water was then diluted with 0.2-μm filtered seawater to obtain duplicate bottles with proportions of 100, 75, 55, 30, and 15% of the experimental water. Dilution series were set up in ten 1.3-L polycarbonate bottles, to which was added a nutrient mixture (10 μM NH_4Cl, 1 μM Na_2HPO_4, 1 nM $FeSO_4$) to ensure that nutrients did not become limiting during the incubation. Two additional undiluted experimental bottles (i.e., 100% bottles) were prepared without nutrients to serve as no-nutrient controls and to assess the net growth rates of protozooplankton. All dispensing was conducted gently to avoid rupturing and damaging the cells. The bottles were incubated on deck for 24 h at ambient sea surface temperatures and screened to ambient light levels with neutral density screening. Subsamples were collected from replicate bottles at 0 and 24 h to determine chl*a* concentrations. For all experiments, a linear regression model was used to plot the best-fit relationship between phytoplankton net growth rate and dilution level (Landry and Hassett, 1982). Phytoplankton growth with nutrient enrichment (μ_n) and grazing rate (g) were defined as the y-intercept and negative slope of the relationship, respectively. Because the intercept of the equation would overestimate phytoplankton growth rate (nutrients were added to these bottles), instantaneous phytoplankton growth rates (μ) were derived from the net phytoplankton growth rate (μ_o) in the undiluted bottles without added nutrients, with addition of the grazing rate (g) of protozooplankton from dilution experiments ($\mu = \mu_o + g$). The impact of protozooplankton grazing on phytoplankton production (%PP) was calculated following Verity et al. (1993): $\%PP\ grazed = 100 \times (1 - \exp(-g))/(1 - \exp(-\mu))$. The net growth rates of protozooplankton were calculated based on the abundances observed in two undiluted water bottles at the beginning and end of the incubations. During incubation, growth or mortality of grazers may have resulted in higher or lower grazing than what is assumed from the dilution factor. In order to evaluate of grazer net growth or loss rate on measurements of μ and g, we used the geometric mean predator density (GMPD) to reassess the experimental output (Gallegos et al., 1996). Phytoplankton growth and protozooplankton grazing rates were calculated by regression of apparent chl*a* growth against GMPD in the incubation bottle (Dolan et al., 2000). Mean ciliates and HDF abundance during the incubation was calculated as (t_0 (ciliate + HDF abundance) × t_{24} (ciliate + HNF abundance))$^{1/2}$, and thus converted to % t_0 grazer abundance (Dolan et al., 2000; Modigh and Franzé, 2009).

2.6. Data analysis

Correlation analyses between protozooplankton and the other measured variables were performed using SPSS (ver. 9.0). Correlation analysis was performed for all sample depths from each station.

3. Results

3.1. Water column properties

The nine stations fell into four groups based on their temperature–salinity characteristics: NPF (stations WS2 to WS5), PF (station WSPF), SPF (stations WSD and WS6), and SACCr (stations WS7 and WS8). Surface temperature gradually decreased from 5.24 °C at the northern part of the transect (station WS2) to 0.23 °C at its southern end (station WS8) (Fig. 2). The sharpest change (from 5 °C to 2 °C),

representing the surface manifestation of the PF, occurred between 56.0°S and 56.5°S. Temperature in the NPF decreased gradually with depth and a thermocline formed at a depth of about 100 m. The subsurface temperature minimum (*T*min, below <0 °C) layer existed around depths of 100–250 m in the southern part of the PF. In the SACCr, approximately constant temperatures were observed above 80 m. Surface salinity in the NPF was generally constant above 300 m. In the SPF, salinity changed significantly from below 50 m to the *T*min depth, developing a shallow pycnocline. In particular, low salinity in surface layers of the SPF might be an effect of meltwater *in situ* and/or from upstream. Salinity in the SACCr was constant within the mixed layer.

Surface concentrations of nitrate exhibited a gradual increase from 22.6 μmol kg^{-1} at the northern part of the transect to 28.4 μmol kg^{-1} at its southern end (Fig. 3). In the SACCr, nitrate concentrations were an average of 6.4 μmol kg^{-1} higher than those in the NPF. Concentrations of silicate exhibited a gradual increase from 12.6 μmol kg^{-1} at the northern part of transect to 104 μmol kg^{-1} at its southern end. Surface silicate concentrations dramatically changed around PF (17.4 to 42.8 μmol kg^{-1}). Surface concentrations of silicate in the SACCr were an average of five times higher than those in the NPF. Vertically, gradients of nitrate and silicate concentration increases with depth were much larger in the southern parts of PF than in the northern parts of PF.

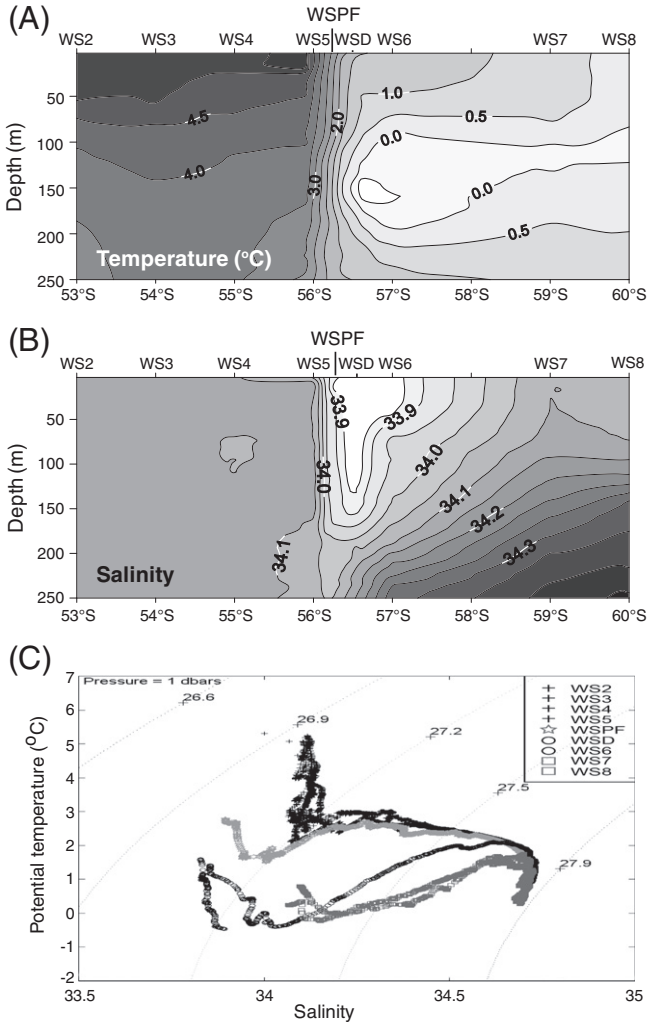

Fig. 2. Vertical section of (A) temperature (°C), (B) salinity, and (C) T–S diagram within the upper 250 m water depth along 52°W transect.

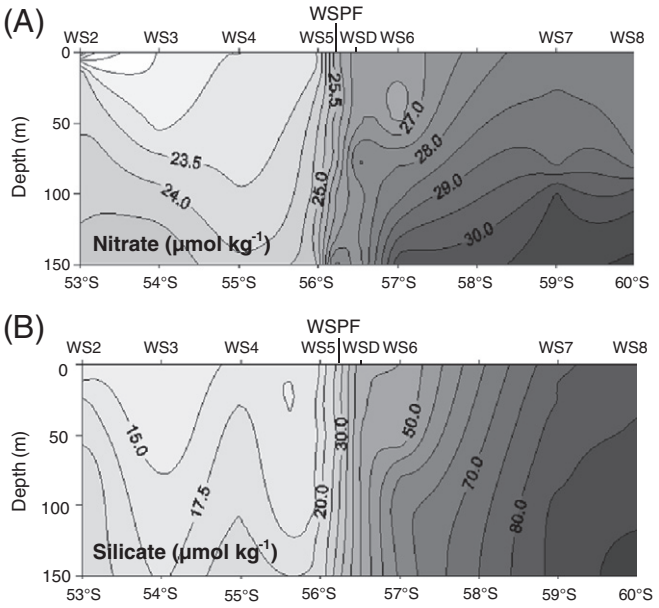

Fig. 3. Vertical section of (A) nitrate (μmol kg^{-1}), and (B) silicate (μmol kg^{-1}) within the upper 150 m water depth along 52°W transect.

3.2. Chlorophyll *a* concentration and phytoplankton communities

In 2001/2002, ocean color imagery from the Sea-viewing Wide Field-of-view Sensor (SeaWiFS) revealed gradual chl*a* accumulation in this region beginning approximately in the third week of December 2001 and peaking in the second week of January 2002 (Fig. 4A). Our study period was earlier than this (third week of December, 2001), and no bloom was observed. Concentrations of chl*a* gradually increased from the NPF (average 0.19 μg L^{-1}) to the SACCr (average 0.56 μg L^{-1}) (Fig. 4B). In the PF, the chl*a* concentration was slightly higher than that in the NPF and SPF. The vertical distribution of chl*a* was more uniform in the NPF, whereas that in the SACCr significantly decreased with depth. The depth-averaged pico-fraction (<3 μm) of chl*a* accounted for 20.1 to 90.4% of total chl*a* and for a greater percentage in the NPF (average 61.2%) (Fig. 4C). The nano-fraction of chl*a* (3–20 μm) constituted 4.0–73.3% of the total chl*a* concentration and formed a greater percentage of the total chl*a* concentration in the SACCr (average 60.3%). Micro-fraction chl*a* (>20 μm) contributed 34.3% on average of the total chl*a* concentration in the PF.

The phytoplankton assemblage varied considerably in both composition and abundance. Phytoplankton in the NPF consisted mostly of eukaryotic picoflagellates (<3 μm) (Fig. 5). The cyanobacteria *Synechococcus* sp. decreased from a high of 300 cells mL^{-1} at the most northern station in the NPF to a low of ~20 cells mL^{-1} at the PF station, disappearing further south. In the PF, diatoms predominated, particularly chain-forming diatoms of the genera *Chaetoceros* spp. and *Fragilariopsis* sp. In the SACCr, the nano-sized flagellate *P. antarctica* was more abundant, together with a *Cryptomonas* sp. and an unidentified autotrophic nanoflagellate (ANF).

3.3. Protozooplankton abundance and community structure

The abundances of protozooplankton components changed both latitudinally and vertically. The abundances of HNF and CNF ranged from 45×10^3 to 2400×10^3 cells L^{-1} and from 5×10^3 to 188×10^3 cells L^{-1}, respectively (Fig. 6). Abundances of HNF and CNF were higher in the NPF than in the southern part of the PF. Abundances of HNF and CNF were greatest in the upper 30 m layer and the 20–50 m layer, respectively, in the NPF. The ciliate assemblage was numerically dominated by naked ciliates, which were further classified into nanociliates

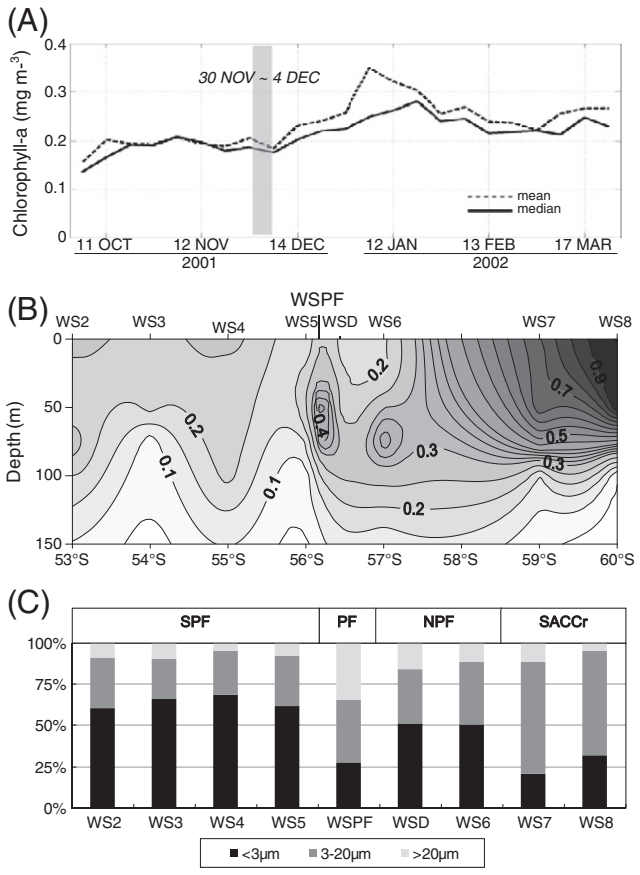

Fig. 4. Spatial and temporal distribution of chlorophyll *a* concentration along 52°W transect. (A) is for time series of the chlorophyll *a* concentration estimated from satellite data around the study region from November 2001 to March 2002. The area is depicted by a white-dotted rectangle in Fig. 1. Shade represents the time of survey, (B) is for the vertical section of chlorophyll *a* concentration and (C) is for the relative percentage of the size-fractionated chlorophyll *a* concentration.

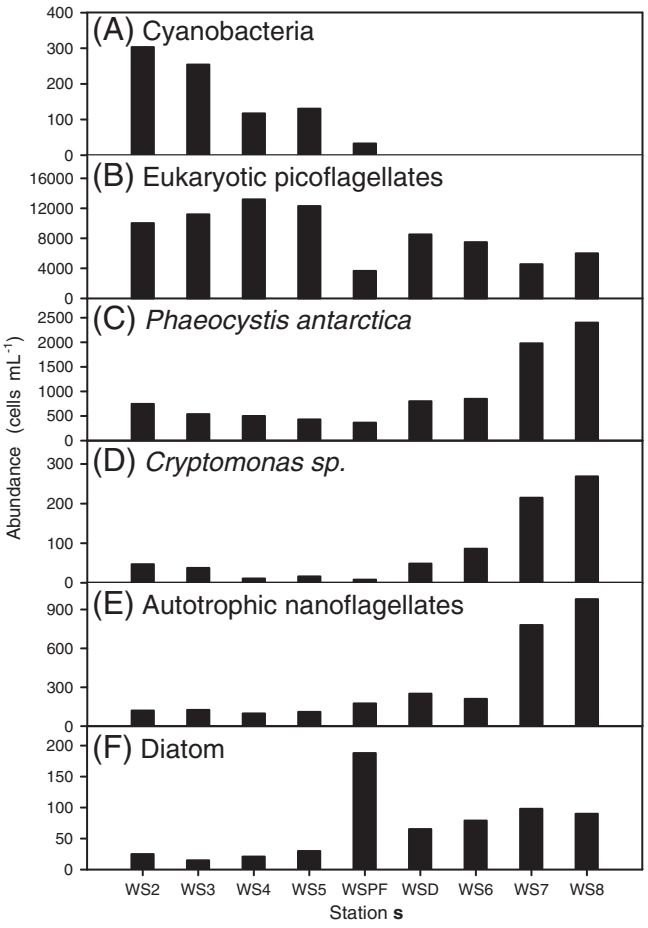

Fig. 5. Distribution of phytoplankton community in subsurface layer along 52°W transect.

(<20 μm) and microciliates (>20 μm), abundances of which ranged from 26 to 13,910 cells L^{-1} and from 20 to 2250 cells L^{-1}, respectively. Nanociliates (10–13 μm in size) were the most abundant in the surface layer in the NPF, whereas microciliate abundance was relatively high in the SACCr. The HDF assemblage was numerically dominated by athecate HDF, which were further classified into nanoHDF (<20 μm) and microHDF (>20 μm), the abundances of which ranged from 110 to 35,020 cells L^{-1} and from 86 to 4234 cells L^{-1}, respectively (Fig. 6). The nanoHDF were most abundant in the SACCr and least abundant in the NPF. In contrast, the abundances of microHDF were relatively high in the PF and SPF.

The depth-integrated protozooplankton biomass from the surface to a depth of 150 m ranged from 443.2 mg C m^{-2} at the northern part of the transect to 934.0 mg C m^{-2} in the PF (Table 1; Fig. 7). The depth-integrated ciliate biomass ranged from 190.2 to 280.4 mg C m^{-2}, and was relatively high in the PF and SACCr. However, ciliate biomass contributed an average of 47.9% to the total biomass in the NPF and less than 30% in the other areas. The depth-integrated HDF biomass ranged from 155.3 to 527.3 mg C m^{-2}, and was significantly higher in the PF and SACCr (average 505.4 mg C m^{-2}) than in the NPF. The HDF biomass contributed an average of 30.1% to the total biomass in the NPF and over 50% in the southern part of PF. Thecate HDF biomass, which was composed mostly of *Protoperidinium* spp., was always low at all stations, although its absolute value was high in the PF. Athecate HDF biomass consisted mainly of *Gyrodinium*, *Amphidinium*, and *Gymnodinium* spp., and accounted for an average of 95% of total HDF biomass. In addition, nanoHDF accounted for 44.1–77.9% of total HDF biomass, with high contributions in the NPF and SPF. The contribution of microHDF to total HDF biomass was greatest in the PF. The depth-integrated HNF biomass ranged from 59.6 to 99.2 mg C m^{-2}. Although the HNF biomass was low in the NPF, the contribution of HNF to total protozooplankton biomass was relatively high in the NPF and PF. CNF biomass and the contribution of CNF to total protozooplankton biomass was the lowest of the entire protozooplankton group. The nanoprotozooplankton population, which consisted largely of HNF, CNH, nanociliates, and nanoHDF, accounted for 39.5–61.8% of total biomass, with its highest contributions being in the NPF (Table 1). In contrast, the contribution of microprotozooplankton to total biomass was highest in the PF, and was much higher in the SACCr.

3.4. Protozooplankton grazing impacts and net growth rates

Instantaneous phytoplankton growth (μ) and protozooplankton grazing rates (g) were derived from dilution experiments (Table 2), and ranged from 0.24 to 0.34 d^{-1} (average, 0.3 ± 0.03 d^{-1}) and 0.18 to 0.26 d^{-1} (average, 0.22 ± 0.04 d^{-1}), respectively. Growth and grazing rates were congruent with those generally reported for the Southern Ocean (Table 3). The average growth rate of phytoplankton without nutrient addition, μ, was statistically indistinguishable from that with nutrients, μ_n (paired *t*-test, $p > 0.05$). Phytoplankton growth did not appear to be nutrient-limited. This level of grazing corresponds to a daily loss of between 66.8 and 94.4% of daily phytoplankton production. Phytoplankton was most heavily grazed in the PF and SPF, with 91.7% of the daily production removed.

The cell-specific net growth rates of protozooplankton were derived from abundance changes in undiluted bottles during the incubation (Fig. 8). Net growth rates of protozooplankton components

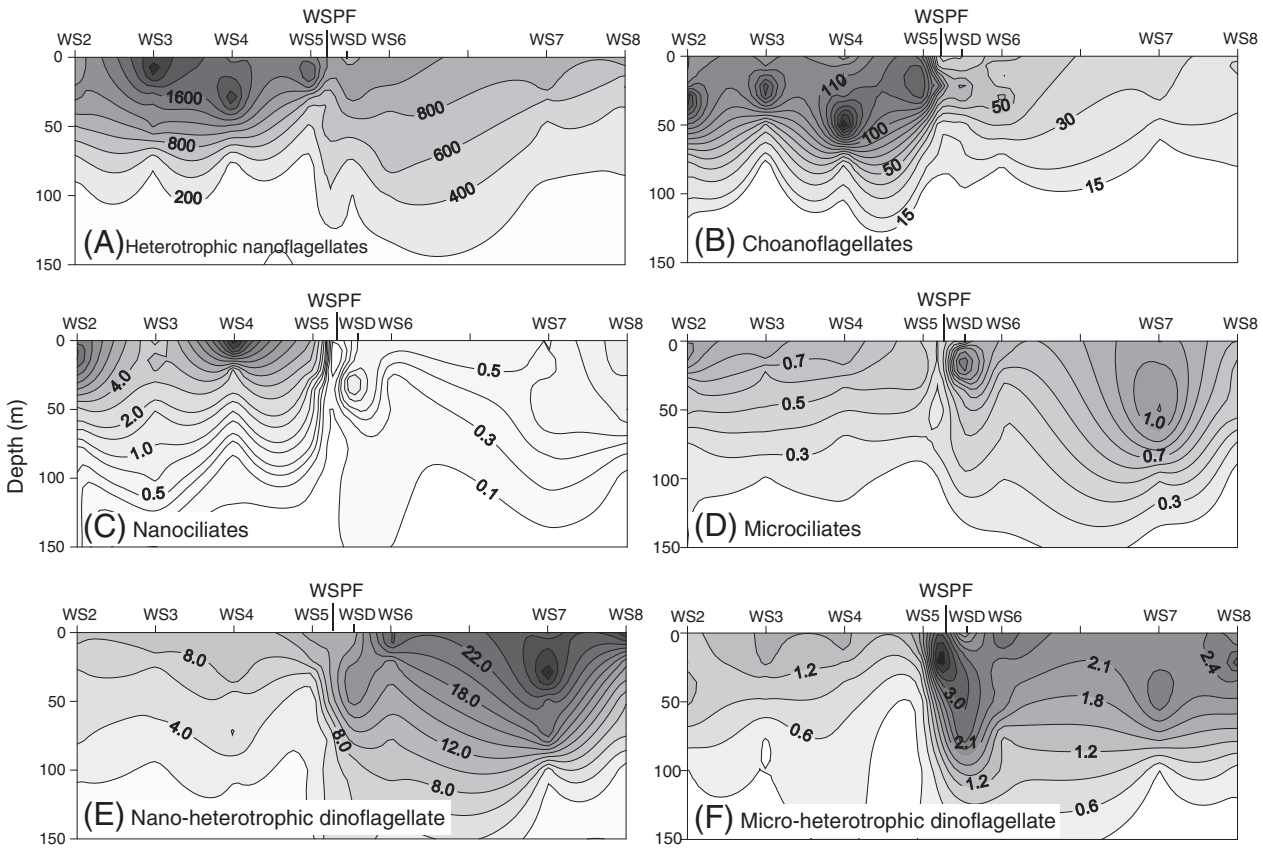

Fig. 6. Distribution of protozooplankton Communities within the upper 150 m water depth along 52°W transect.

showed spatial patterns according to composition and size structures. The net growth rate of HNF, including CNF, was generally low, ranging from −0.31 to 0.1 d^{-1}. Net growth rates of nanociliates and microciliates ranged from −0.11 to 0.63 d^{-1} and from 0.11 to 0.23 d^{-1}, respectively, and were much higher in the NPF than in other areas. Growth rates of nanoHDF and microHDF ranged from −0.11 to 0.41 d^{-1} and from −0.01 to 0.28 d^{-1}, respectively.

3.5. Correlation relationships among protozooplankton, phytoplankton, and physical factors

Table 4 shows the correlations among the protozooplankton community, the relative percent of size-fractionated chl*a* concentration, phytoplankton composition, and physical parameters. All groups of protozooplankton (except microciliates) were significantly correlated with temperature. NanoHDF was positively correlated with nano/

Table 1
Carbon biomass (mgC m^{-2}) of protozooplankton groups integrated down to 150 m. HNF: heterotrophic nanoflagellates, CNF: choanoflagellates, HDF: heterotrophic dinoflagellates, PZ: protozooplankton.

Region stations	North of PF WS2-WS5	PF WSPF	South of PF WSD, WS6	SACCr WS7, WS8
Nanoprozooplankton				
HNF	62.6	99.4	75.3	73.9
CNF	40.2	19.4	18.0	10.2
HDF	97.8	225.9	283.5	276.2
Ciliates	101.1	8.9	26.4	15.1
Total	301.7	353.6	403.2	375.4
Microprotozooplankton				
HDF	63.8	299.9	113.0	233.2
Ciliates	136.3	280.5	201.0	272.8
Total	200.0	580.4	314.0	506.0
Total PZ	501.7	934.0	717.2	881.4
Nano PZ/total PZ (%)	60.1	37.9	56.2	42.6

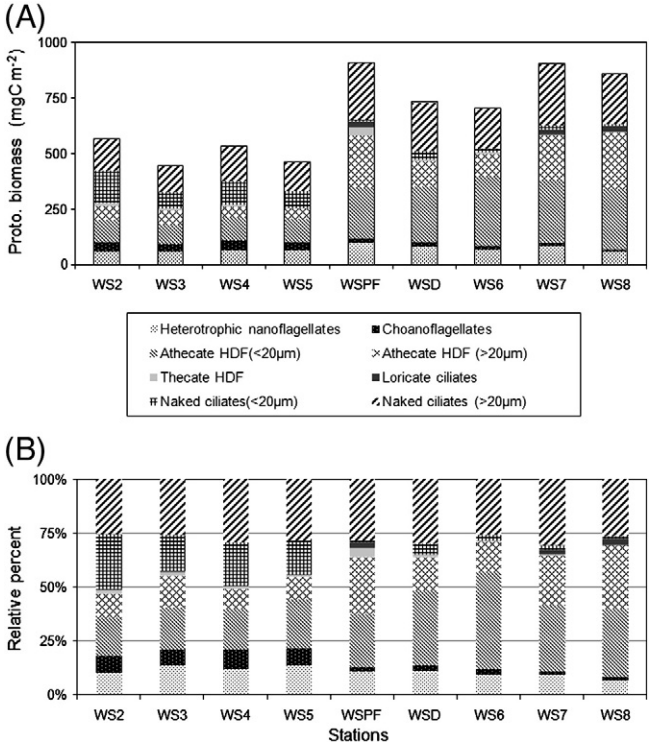

Fig. 7. Carbon biomass of protozooplankton along 52°W transect. (A) is for cumulative carbon biomass, and (B) is for relative percent of protozooplankton community.

Table 2
Summary parameters and grazing impact by protozooplankton at 10 m derived from dilution experiments. μ_n: phytoplankton growth rate, μ: phytoplankton growth rate without added nutrients, g: microzooplankton grazing rates, PP (%): daily phytoplankton production grazed, r^2: correlation coefficient, $p<0.05$, PP_G (%): adjusted daily phytoplankton production grazed for grazer gradient represented by GMPD.

Station	Initial Chl*a* ($\mu g\ L^{-1}$)	Temperature (°C)	μ (d^{-1})	μ_n (d^{-1})	g (d^{-1})	PP (%)	r^2	PP_G (%)
WS2	0.20	5.24	0.32	0.31	0.22	72.16	0.79	68.00
WS3	0.18	5.09	0.30	0.32	0.20	66.19	0.78	62.30
WS4	0.20	5.08	0.34	0.33	0.24	70.50	0.74	70.20
WS5	0.14	5.07	0.30	0.28	0.19	66.76	0.88	66.08
WSPF	0.27	2.77	0.31	0.29	0.28	94.40	0.81	90.90
WS6	0.19	1.40	0.32	0.28	0.26	89.17	0.90	87.37
WS7	0.61	0.78	0.26	0.25	0.20	79.17	0.92	78.22
WS8	0.78	0.31	0.24	0.23	0.18	77.20	0.85	78.54

Tchl*a*, *P. antarctica* and *Cryptomonas* sp., whereas microHDF was positively correlated with micro/Tchl*a*, nano/Tchl*a*, and diatoms. Microciliates were positively correlated with nano/Tchl*a*, and nanociliates were positively correlated with cyanobacteria and picoflagellates. We found a strong correlation between total protozooplankton biomass and each group of size-fractionated phytoplankton group.

4. Discussion

Our study of the mesoscale distribution of the protozooplankton community and its grazing impact in the western Scotia Sea demonstrated that (i) the community and size structure of protozooplankton generally followed the spatial dynamics and size structure of the phytoplankton community, (ii) ciliates and HDF were significant components of protozooplankton populations in different water masses, and (iii) the proportion of phytoplankton grazed by protozooplankton varied in relation to the community structure of both phytoplankton and protozooplankton, with protozooplankton capable of consuming an average of 76.9% of daily phytoplankton production.

In the open waters of the Southern Ocean, plankton communities differ markedly north and south of the PF due to the strong physicochemical gradients in the region of the front (Froneman and Pakhomov, 1998; Klass, 1997; Pakhomov et al., 1994). Although previous studies have investigated protozooplankton communities and grazing in the Southern Ocean (Becquevort et al., 2000; Klass, 1997; Safi et al., 2007; Selph et al., 2001), this is the first study of the protozooplankton community and its herbivorous activity in the western Scotia Sea during the spring. Our results showed that marked alterations in the community composition and abundance of phytoplankton and protozooplankton were associated with marked changes in the physicochemical environments of different water masses. The most pronounced gradient found in this study was the substantially greater macronutrient and plankton biomass in the southern parts of the PF as compared to that to its north. The chl*a* concentration increased from the relatively warmer NPF waters, with lower concentrations of macro-nutrients, toward the colder SACCr waters, with higher concentrations of macro-nutrients. Picophytoplankton, including cyanobacteria and eukaryotic picoflagellates, dominated in the NPF, whereas nanophytoplankton, such as *P. antarctica* and *Cryptomonas* sp., dominated in the SACCr (Fig. 5). Cyanobacteria were not observed in water cooler than 2 °C in the southern part of PF. In the southern part of PF, picophytoplankton consisted of eukaryotic picoflagellates. In the Atlantic and Southern Oceans, there is a general trend of decreasing cyanobacteria abundance with increasing latitude

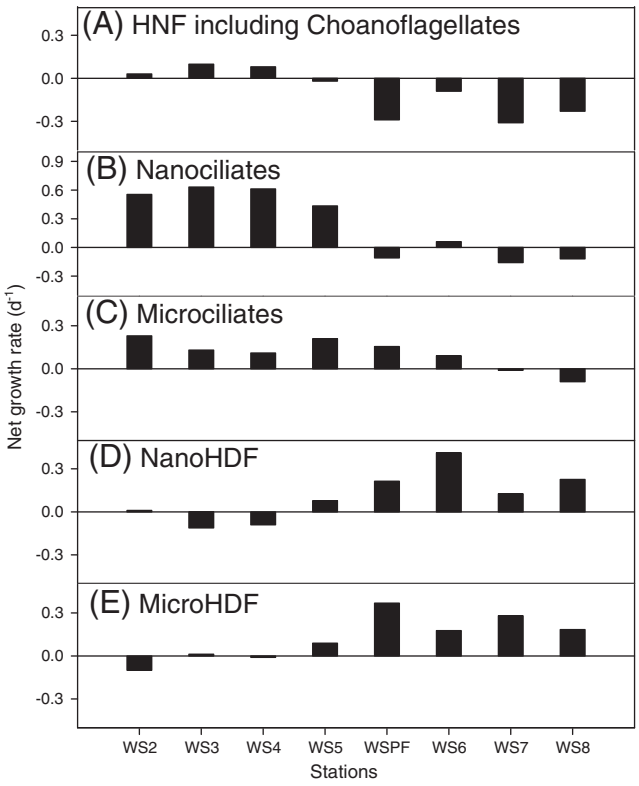

Fig. 8. Cell specific net growth rates for protozooplankton community in undiluted seawater during incubation of dilution experiments. (A) is for heterotrophic nanoflagellates including choanoflagellates, (B) is for nanociliates, (C) is for microciliates, (D) is for nano-heterotrophic dinoflagellates, and (E) is for micro-heterotrophic dinoflagellates.

Table 3
Regional comparisons of protozooplankton herbivory reported in the Southern Ocean. PP (%): potential phytoplankton production grazed. The numbers of parentheses refer to average value.

Study area	Study periods	Chl*a* ($\mu g\ L^{-1}$)	Growth rate (d^{-1})	Grazing rate (d^{-1})	PP (%)	Reference
Eastern Altantic Sector	1997. 12–1998. 1	1.52–2.09	0.04–0.28	–	11.1–34.5	Froneman (2004)
South of Tasmania (46°S–67°S, 140°E–145°E)	2001. 11–12	0.1–0.68	0.19–0.89 (0.44)	0.18–0.57 (0.35)	45–127 (91)	Safi et al. (2007)
57°S–61°S, 170°W	1997. 12	0.17–1.5	0.8–1.0 (0.61)	0.03–0.55 (0.34)	40–69 (56)	Selph et al. (2001)
57°S–61°S, 170°W	1997. 11	0.2–0.9	0.08–0.3 (0.2)	0.1–0.23 (0.16)	(79.0)	Landry et al. (2001)
Atlantic sector (35°S–70°S, 0–20°W)	1993	1–2 0.09–2.07	0.06–1.87	0–0.58	0–59 (24.1)	Froneman and Perissinotto (1996)
Bellingshausen sea	1992. 11–12	0.05–1.4	–	–	21–271	Burkill et al. (1995)
Indo Pacific and Atlantic sector	1994. 12–1995. 1	0.08–2.28	0.1–0.4	0–0.3	0–333 (104)	Tsuda and Kawaguchi (1997)
South of Tasmania (Sub-Antarctic zone)	2007. 1–2	0.28–2.21	0.02–1.02 (0.4)	0.12–1.39 (0.53)	47–82 (64.2)	Pearce et al. (2011)
Southern Ocean	–	(0.62)	(0.44)	(0.16)	(59.2)	Calbet and Landry (2004)
Western Scotia Sea	2001. 12	0.09–0.90	0.24–0.34 (0.30)	0.18–0.26 (0.22)	66.8–94.4 (76.9)	This study

Table 4
Pearson's correlation coefficients between protozooplankton, and phytoplankton and physical factors. HNF: heterotrophic nanoflagellates, CNF: choanoflagellates, HDF: heterotrophic dinoflagellates, PZ: protozooplankton, ANF: autotrophic nanoflagellates. Tchl*a*: total chlorophyll *a*, sample number (n) is 72 except of phytoplankton community **in bold** ($n=8$).

	HNF (cells mL^{-1})	CNF (cells mL^{-1})	NanoHDF (cells mL^{-1})	MicroHDF (cells mL^{-1})	Nanociliates (cells mL^{-1})	Microciliates (cells mL^{-1})	Total PZ (μgC L^{-1})
Temperature (°C)	0.360**	0.664***	−0.371**	−0.272*	0.533***	0.026	0.006
Salinity	−0.167	0.086	−0.352**	−0.641***	0.211	−0.113	−0.310**
Total chl*a* (μgC L^{-1})	0.032	−0.118	0.619***	0.372**	−0.026	0.305*	0.470***
Net/Tchl*a* (%)	0.111	−0.031	0.068	0.435***	−0.078	0.061	0.284*
Nano/Tchl*a* (%)	0.211	0.111	0.596***	0.573***	0.068	0.322*	0.584***
Pico/Tchl*a* (%)	−0.111	−0.079	−0.556***	−0.727***	−0.018	−0.312*	−0.658***
Cyanobacteria[a]	0.203	0.795*	−0.753*	−0.366	0.691*	0.503	–
Picoflagellates[a]	0.388	0.886**	−0.645	−0.394	0.699*	0.087	–
Phaeocystis antarctica[a]	−0.468	−0.553	0.794*	−0.217	−0.307	0.141	–
***Cryptomonas* sp.**[a]	−0.329	−0.634	0.856**	0.009	−0.419	0.014	–
ANF[a]	−0.353	−0.796	0.948***	0.178	−0.632	−0.143	–
Diatom[a]	0.112	−0.230	−0.107	0.700*	−0.504	−0.411	–

[a] Units: cells mL^{-1}.
* Significant at the $P<0.05$ level.
** Significant at the $P<0.005$ level.
*** Significant at the $P<0.0005$ level.

and decreasing temperature, and a marked predominance of eukaryotic picoplankton in cold water (Doolittle et al., 2008; Ishikawa et al., 2002; Murrphy and Haugen, 1985). The PF was characterized by high abundance of microphytoplankton, including chain-forming diatoms, as reported previously (Brown and Landry, 2001).

The protozooplankton community consisted of a range of taxa similar to those that have been reported previously from parts of the Southern Ocean (Becquevort et al., 2000; Froneman and Perissinotto, 1996; Garrison and Buck, 1989; Safi et al., 2007). Nanociliates declined in importance from the relatively warm NPF waters toward the colder SACCr waters. Nanociliates correlated well with temperature, cyanobacteria, and eukaryotic picoflagellate abundance. However, the general decline of nanociliates toward the southern part of the PF may reflect changes in picophytoplankton structure and temperature. This result is also supported by the high growth rates of nanociliates in the NPF. Our result is similar to those of previous studies conducted in the Weddell Sea and south of Tasmania (Garrison and Buck, 1989; Safi et al., 2007). However, the peak abundance of nanociliates (13,910 cells L^{-1}; Fig. 6) was observed at station WS4, and to our knowledge, such figures have never previously been reported for the open waters of the Southern Ocean (Fig. 6). The abundance of microciliates was relatively high in the SACCr and correlated well with nano/Tchl*a*, suggesting that this group preferred to graze on nanophytoplankton. Therefore, the spatial distribution in the size composition of ciliates was in agreement with phytoplankton size community and biomass distribution. In contrast to ciliates, HDF populations increased in importance from the relatively warm NPF waters toward the colder SACCr waters, and were the dominant component of protozooplankton biomass (>50%) in the southern part of PF (Fig. 7), as reported previously in the Southern Ocean (Archer et al., 1996; Becquevort et al., 2000; Nöthig et al., 1991; Pearce et al., 2011). In particular, nanoHDF accounted for 44.1–77.9% of total HDF biomass, with high contributions everywhere, except in the PF (Fig. 7). During this study, nanoHDF was positively correlated with nano/Tchl*a* and nanophytoplankton (ANF, *Phaeocystis*, *Cryptomonas*), whereas microHDF was positively correlated with micro/Tchl*a*, nano/Tchl*a*, and diatoms. These results imply that food supply may be the most important factor controlling the spatial dynamics of nano- and microHDF populations. Several previous studies have reported that HNF are usually the dominant protozooplankton in HNLC waters of the Southern Ocean (Becquevort et al., 1992; Hall et al., 2004; Kivi and Kuosa, 1994; Safi et al., 2007). Although the abundances of HNF and CNF in this study were similar to those reported for parts of the Southern Ocean, they constituted a minor group of protozooplankton, accounting for <15% of total protozooplankton biomass in this area. HNF and CNF have been identified as potentially important grazers of heterotrophic bacteria and picophytoplankton (Becquevort et al., 2000; Calbet et al., 2001; Guillou et al., 2001). We found significant correlations between CNF and picophytoplankton, despite the lack of a correlation between HNF and picophytoplankton. During the study period, bacterial abundance increased from the NPF toward the SACCr, and showed a distribution pattern similar to that of HNF (Hyun and Yang, 2003). Therefore, HNF may be more important grazers of heterotrophic bacteria than of picophytoplankton. These results imply that CNF, may contribute much more than HNF to protozooplankton herbivory. Conclusively, the significant correlation between the protozooplankton population and phytoplankton composition may be indicative of the spatial dynamics of protozooplankton responding to size and community composition of phytoplankton.

The importance of protozooplankton as consumers of phytoplankton in the Southern Ocean has largely been derived from investigations employing dilution experiments (Table 3). The grazing impact of protozooplankton on phytoplankton was substantial in the present study area, accounting for an average of 75.2% of daily phytoplankton production. Although some studies have reported low grazing by protozooplankton at times in parts of the Southern Ocean (Caron et al., 2000; Froneman, 2004; Froneman and Perissinotto, 1996), our results are in the same range as those of similar studies conducted during spring in the Southern Ocean (Table 3, Landry et al., 2001; Safi et al., 2007). In the PF, the marked impact of grazing by protozooplankton, with their higher diatom abundance, coincided with a high protozooplankton biomass, especially microHDF (Fig. 9). This is in contrast to other studies, which showed that protozooplankton were unable to control the growth of larger phytoplankton (>20 μm) in the Southern Ocean (Froneman, 2004; Froneman and Perissinotto, 1996; Safi et al., 2007). HDF can consume large diatoms because they exhibit complex feeding behaviors and mechanisms that enable them to feed on larger prey (Hansen and Calado, 1999; Jeong et al., 2010). However, the high grazing in the PF may be interpreted as the result of high microHDF growth rates as well as their high abundance, particularly *Protoperidinium* spp. (Fig. 8, 9). The second highest impact of protozooplankton grazing in the SPF also coincided with a high nanoHDF biomass and picophytoplankton dominance. The greater grazing by protozooplankton in the SPF compared to the NPF, which had similar properties to the SPF in terms of phytoplankton size structure, is probably due to differences in protozooplankton composition between the two areas. The abundance and net growth of nanociliates were highest in the NPF, whereas those of nanoHDF were highest in the SPF (Figs. 6, 8). This result is supported by a previous study, which showed that nanoHDF

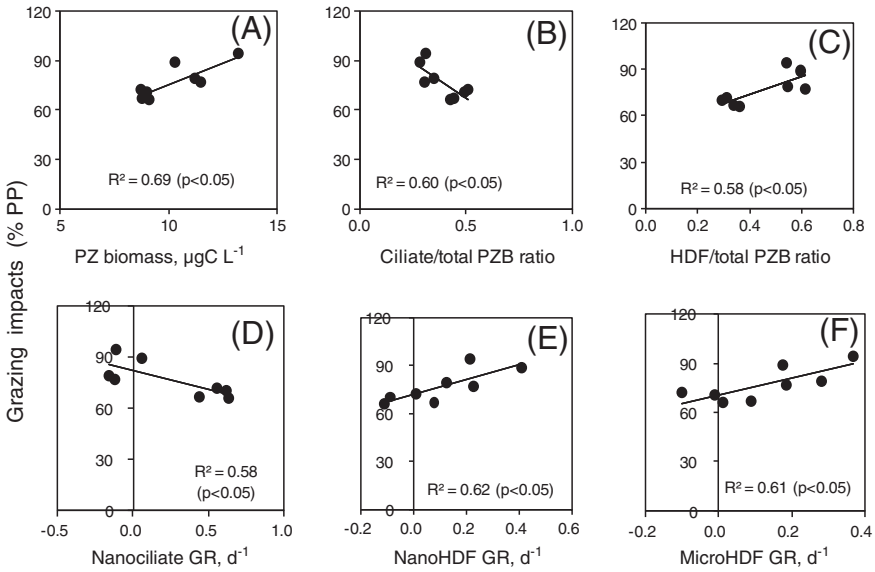

Fig. 9. Relationship between grazing impacts of protozooplankton and (A) initial protozooplankton biomass (PZB), (B) ciliate/total protozooplankton biomass ratio, (C) HDF/total protozooplankton biomass ratio, (D) growth rates (GR) of nanociliates, (E) growth rates of nano-heterotrophic dinoflagellates, and (F) growth rates of micro-heterotrophic dinoflagellates.

ingested, on average, two times more phototrophic flagellates than did nanociliates in the Southern Ocean (Becquevort et al., 2000). Although high proportions of nano- and picophytoplankton can strongly influence the effects of protozooplankton grazing on phytoplankton in HNLC regions (Froneman and Perissinotto, 1996; Safi et al., 2007), our results suggest that microphytoplankton were also being controlled by protozooplankton grazing.

Changes in protozooplankton abundance were observed during dilution incubations. The net growth of protozooplankton in an undiluted bottle will be the sum of increases due to intrinsic growth and losses due to death or predation from within the protozooplankton community. The growth response of protozooplankton in dilution experiments can provide insight into trophic structure and efficiency of the microbial food web (First et al., 2007). In this study, a positive net growth rate of HDF and microciliates was observed in the southern part of PF (Fig. 8). Protozooplankton abundance increased during incubations, indicating that grazer dynamics are an inherent component of dilution experiments (First et al., 2007). Also, the negative growth rates of HNF, CNF, and nanociliates in the southern part of PF indicate that they sustained substantial grazing pressure from the microprotozooplankton. This result is consistent with those of Strom et al. (2007), who reported that net protozooplankton growth rate decreased with decreasing protozooplankton cell size. Therefore, changes in grazer abundance can provide clues as to trophic interactions within protozooplankton during incubation. It has been argued that changes in grazer abundance during dilution incubation may result in results that are artifacts (Dolan et al., 2000; Modigh and Franzé, 2009). Grazer abundance increases in undiluted water and decreases in highly dilute water may be common and result in uncertainty in measured protozooplankton grazing rates. Modigh and Franzé (2009) suggested that if the growth and mortality of grazers in dilution series are not considered, microzooplankton grazing impact may be either underestimated (at low phytoplankton growth rates), or overestimated under more productive conditions. Although grazer abundance changed during dilution experiments, adjusting PP_G (%) for the actual grazer gradient (represented by GMPD) did not cause significant deviation from the nominal dilution gradient (Table 2). Therefore, actual grazing impacts could be driven by changes in the protozooplankton community composition and abundance, since the biomass of specific grazer taxa wax and wane in concert with variations in prey composition.

Although dilution experiments have become the standard method for estimating the grazing of protozooplankton, their reliability has been questioned. Dolan and McKeon (2005) advanced the hypothesis that dilution experiments may overestimate microzooplankton grazing, as shown by unrealistically high clearance rates. These authors suggested a maximum ciliate clearance in the field of 10 μL ciliates^{-1} h^{-1}. We calculated average individual clearance rates based on grazing rate and protozooplankton abundance. Assuming they were the only grazers, the clearance rate by ciliates ranged from 1.0 to 10.6 μL ciliates^{-1} h^{-1}, with an average of 5.9 μL ciliates^{-1} h^{-1}. Considering HDF, the estimated clearance rates ranged from 2.7 to 10.8 μL HDF^{-1} h^{-1}, with an average of 5.7 μL HDF^{-1} h^{-1}. The clearance rates estimated in this study indicate that the grazing rates obtained in our dilution experiments may be realistic.

In summary, our results suggest that changes of dominant protozooplankton group (ciliate and HDF) in the different water mass play vital roles in the impact of protozooplankton grazing on the phytoplankton. Therefore, this study has identified some key changes and linkages that occur in microbial food webs along environmental gradients in the western Scotia Sea. In addition, our estimate of protozooplankton grazing impact (i.e., an average of 76.9% of daily phytoplankton production) is greater than that reported elsewhere (59.2%) for the Southern Ocean (Calbet and Landry, 2004). Previous studies have reported that grazing by copepods was low and accounted for less than 1% of primary production in the PF and ACC–Weddell Gyre Boundary (Dubischar and Bathmann, 1997). Therefore, our results demonstrate that protozooplankton were the major consumers of diverse phytoplankton communities, and that protozooplankton grazing is one of the most important loss processes affecting phytoplankton biomass and composition during spring in the western Scotia Sea.

Acknowledgments

The authors thank the captain and crew of the *R/V Yuzhmorgeologia* who were most helpful in all shipboard operations. The authors would also like to thank the anonymous reviewers for their thoughtful suggestions that significantly improved the quality of the paper. This work was supported by KOPRI projects PP12010 and PM11080. **[SS]**

References

Archer, S.D., Leakey, R.J.G., Burkill, P.H., Sleigh, M.A., 1996. Microbial dynamics in coastal waters of East Antarctica; herbivory by heterotrophic dinoflagellates. Mar. Ecol. Prog. Ser. 139, 239–255.

Becquevort, S., Mathot, S., Lancelot, C., 1992. Interactions in the microbial community of the marginal ice zone of the northwestern Weddell Sea through size distribution analysis. Polar Biol. 12, 211–218.

Becquevort, S., Menon, P., Lancelot, C., 2000. Differences of the protozoan biomass and grazing during spring and summer in the Indian sector of the Southern Ocean. Polar Biol. 23, 309–310.

Brandon, M.A., Naganobu, M., Demer, D.A., Chernyshkov, P., Trathan, P.N., Thorpe, S.E., Kameda, T., Berezhinskiy, O.A., Hawker, E.J., Grant, S., 2004. Physical oceanography in the Scotia Sea during the CCAMLR 2000 survey, austral summer 2000. Deep-Sea Res. Part II 51, 1301–1321.

Brown, S.L., Landry, M.R., 2001. Microbial community structure and biomass at the peak of a summer bloom at the Polar Front along 170°W. Deep-Sea Res. Part II 48, 2039–2058.

Brown, S.L., Landry, M., Neveux, J., Dupouy, C., 2003. Microbial community abundance and biomass along a 180° transect in the equatorial Pacific during an El Nino–Southern oscillation cold phase. J. Geophys. Res. 108 (C12), 8139, http://dx.doi.org/10.1029/2001JC000817.

Bøsheim, K.Y., Bratbak, G., 1987. Cell volume to cell carbon conversion factors for a bacterivorus *Monas* sp. enriched from sea waters. Mar. Ecol. Prog. Ser. 36, 171–175.

Burkill, P.H., Edwards, E.S., Sleigh, M.A., 1995. Microzooplankton and their role in controlling phytoplankton growth in the marginal ice zone of the Bellingshausen Sea. Deep-Sea Res. Part II 42, 1277–1299.

Calbet, A., Landry, M.R., 2004. Phytoplankton growth, microzooplankton grazing and carbon cycling in marine systems. Limnol. Oceanogr. 49, 51–57.

Calbet, A., Landry, M.R., Nunnery, S., 2001. Bacteria–flagellate interactions in the microbial food web of the oligotrophic subtropical North Pacific. Aquat. Microb. Ecol. 23, 283–292.

Caron, D.A., Dennett, M.R., Lonsdale, D.J., Moran, D.M., Shalapyonok, L., 2000. Microzooplankton herbivory in the Ross Sea, Antarctica. Deep-Sea Res. Part II 47, 3249–3272.

Dolan, J.R., Gallegos, C.L., Moigis, A., 2000. Dilution effects on microzooplankton in dilution grazing experiments. Mar. Ecol. Prog. Ser. 200, 127–139.

Dolan, J., McKeon, K., 2005. The reliability of grazing rate estimates from dilution experiments: have we over-estimated rates of organic carbon consumption by microzooplankton? Ocean Sci. 1, 1–7.

Doolittle, D.F., Li, W.K.W., Michelle Wood, A., 2008. Wintertime abundance of picoplankton in the Atlantic sector of the Southern Ocean. Nova Hedwigia, Beiheft, 133, pp. 147–160.

Dubischar, C.D., Bathmann, U.V., 1997. Grazing impact of copepods and salps on phytoplankton in the Atlantic sector of the Southern Ocean. Deep-Sea Res. Part II 44, 415–433.

Edler, L., 1979. Phytoplankton and chlorophyll recommendations for biological studies in the Baltic Sea. Balt. Mar. Biol. 13–25.

First, M.R., Lavrentyev, P.J., Jochem, F.J., 2007. Patterns of microzooplankton growth in dilution experiments across a trophic gradient: implications for herbivory studies. Mar. Biol. 151, 1929–1940.

Froneman, P.W., 2004. Protozooplankton community structure and grazing impact in the eastern Atlantic sector of the Southern Ocean in austral summer 1998. Deep-Sea Res. Part II 51, 2633–2643.

Froneman, P.W., Perissinotto, R., 1996. Structure and grazing of the microzooplankton communities of the subtropical convergence and a warm core eddy in the Atlantic sector of the Southern Ocean. Mar. Ecol. Prog. Ser. 135, 237–245.

Froneman, P.W., Pakhomov, E.A., 1998. Biogeographic study of the planktonic communities of the Prince Edward Islands (Southern Ocean). J. Plankton Res. 20, 653–669.

Fortier, L., Lefevre, J., Legendre, L., 1994. Export of biogenic carbon to fish and to the deep-ocean the role of large planktonic microphages. J. Plankton Res. 16, 809–839.

Gallegos, C.L., Vant, W.N., Safi, K.A., 1996. Microzooplankton grazing of phytoplankton in Manukau Harbour, New Zealand. N. Z. J. Mar. Freshw. Res. 30, 423–434.

Garrison, D.L., Buck, K.R., 1989. Protozooplankton in the Weddell Sea, Antarctica: abundance and distribution in the ice-edge zone. Polar Biol. 9, 341–351.

Garrison, D.L., 1991. An overview of the abundance and role of protozooplankton in Antarctic waters. J. Mar. Syst. 2, 317–331.

Guillou, L., Jacquet, S., Chrétiennot-Denet, M., Vaulot, D., 2001. Grazing impact of two small heterotrophic flagellates on *Prochlorococcus* and *Synechococcus*. Aquat. Microb. Ecol. 26, 201–207.

Hansen, P.J., Calado, A.J., 1999. Phagotrophic mechanisms and prey selection in free-living dinoflagellates. J. Eukaryot. Microbiol. 46, 382–389.

Hall, J.A., Safi, K.A., Cummings, A., 2004. Role of microzooplankton grazers in the subtropical and subantarctic waters to the east of New Zealand. N. Z. J. Mar. Freshw. Res. 38, 91–101.

Holm-Hansen, O., Naganobu, M., Kawaguchi, S., Kameda, T., Krasovski, I., Tchernyshkov, P., Prdiddle, J., Korb, R., Brandon, M., Demer, D., Hewitt, R.P., Kahru, M., Hewes, C.D., 2004. Factors influencing the distribution, biomass, and productivity of phytoplankton in the Scotia Sea and adjoining waters. Deep-Sea Res. Part II 51, 1333–1350.

Hyun, J.H., Yang, E.J., 2003. Distribution and structure of the microbial community in the Weddell Sea and Bransfield Strait. Oceanographic studies on Antarctic marine living resource and ecosystem, pp. 241–271. BSPP 02104-00-1511-7 (in Korean with English Abstracts).

Ishikawa, A., Wright, S.W., van den Enden, R., Davidson, A.T., Marchant, H.J., 2002. Abundance, size structure and community composition of phytoplankton in the Southern Ocean in the austral summer 1999/2000. Polar Biosci. 15, 11–26.

Jeong, H.J., Yoo, Y.D., Kim, J.S., Seong, J.A., Kang, N.S., Kim, T.H., 2010. Growth, feeding and ecological roles of the mixotrophic and heterotrophic dinoflagellates in marine planktonic food webs. Ocean Sci. J. 45, 65–91.

Kattner, G., 1999. Storage of dissolved inorganic nutrients in seawater: poisoning with mercuric chloride. Mar. Chem. 67, 61–66.

Kawaguchi, S., Siegel, V., Litvinov, F., Loeb, V., Watkins, J., 2004. Salp distribution and size composition in the Atlantic sector of the Southern Ocean. Deep-Sea Res. Part II 51, 1369–1381.

Klass, M., 1997. Microprotozooplankton distribution and their potential grazing impact in the Antarctic Circumpolar Current. Deep-Sea Res. Part II 44, 375–393.

Kivi, K., Kuosa, H., 1994. Late winter microbial communities in the western Weddell Sea (Antarctica). Polar Biol. 14, 389–399.

Korb, R.E., Whitehouse, M.K., Thorpe, S.E., Gordon, M., 2005. Primary production across the Scotia Sea in relation to the physico-chemical environment. J. Mar. Syst. 57, 231–249.

Landry, M.R., Hassett, R.P., 1982. Estimating the grazing impact of marine microzooplankton. Mar. Biol. 67, 283–288.

Landry, M.R., Brown, S.L., Selph, K.E., Abbott, M.R., Letelier, R.M., Christensen, S., Bidigare, R.R., Casciotti, K., 2001. Initiation of the spring phytoplankton increase in the Antarctic Polar Front Zone at 170°W. J. Geophys. Res. 106 (C7), 13,903–13,915.

Menden-Deuer, S., Lessard, E.J., 2000. Carbon to volume relationships for dinoflagellates, diatoms, and other protist plankton. Limnol. Oceanogr. 45, 569–579.

Meredith, M.P., Watkins, J.L., Murphy, E.J., Ward, P., Bone, D.G., Thorpe, S.E., Grant, S.A., Ladkin, R.S., 2003. Southern ACC Front to the northeast of South Georgia: pathways, characteristics, and fluxes. J. Geophys. Res. 108 (C5), 3162, http://dx.doi.org/10.1029/2001JC001227.

Modigh, M., Franzé, G., 2009. Changes in phytoplankton and microzooplankton populations during grazing experiments at a Mediterranean costal site. J. Plankton Res. 31, 853–864.

Moore, J.K., Abbott, M.R., 2002. Surface chlorophyll concentrations in relation to the Antarctic polar front: seasonal and spatial patterns from satellite observations. J. Mar. Syst. 37, 69–86.

Moore, J.K., Abbott, M.R., Richman, J.G., 1997. Variability in the location of the Antarctic Polar Front (90°–20°W) from satellite sea surface temperature data. J. Geophys. Res. 102 (c13), 27,825–27,833.

Murphy, E.J., Watkins, J.L., Trathan, P.N., Reid, K., Meredith, M.P., Thorpe, S.E., Johnston, N.M., Clarke, A., Tarling, G.A., Collins, M.A., Forcada, J., Shreeve, R.S., Atkinson, A., Korb, R., Whitehouse, M.J., Ward, P., Rodhouse, P.G., Enderlein, P., Hirst, A.G., Martin, A.R., Hill, S.L., Staniland, I.J., Pond, D.W., Briggs, D.R., Cunningham, N.J., Fleming, A.H., 2007. Spatial and temporal operation of the Scotia Sea ecosystem: a review of large-scale links in a krill centred food web. Philos. Trans. R. Soc. London, Ser. B 362, 113–148.

Murrphy, L.S., Haugen, E.M., 1985. The distribution and abundance of phototrophic ultraplankton in the North Atlantic. Limnol. Oceanogr. 30, 47–58.

Nowlin Jr., W.D., Whitworth III, T., Pillsburry, R.D., 1977. Structure and transport of the Antarctic Circumpolar Current at Drake Passage from short-term measurements. J. Phys. Oceanogr. 7, 778–802.

Nöthig, E.M., Bodungen, B., Sui, Q., 1991. Phyto-and protozooplankton biomass during austral summer in surface waters of the Weddell Sea and vicinity. Polar Biol. 11, 293–304.

Orsi, A.H., Whitworth III, T., Nowlin, W.D., 1995. On the meridional extent and fronts of the Antarctic Circumpolar Current. Deep-Sea Res. Part I 42, 641–673.

Pakhomov, E.A., Perissinotto, R., McQuaid, C.D., 1994. Comparative structure of the macrozooplankton/micronekton communities of the Subtropical and Antarctic Polar Fronts. Mar. Ecol. Prog. Ser. 111, 155–169.

Parson, T.R., Maita, Y., Lalli, C.M., 1984. A Manual of Chemical and Biological Methods for Seawater Analysis. Pergamon Press, Oxford. 173 pp.

Pearce, I., Davidson, A.T., Thomson, P.G., Wright, S., van den Enden, R., 2011. Marine microbial ecology in the sub-Antarctic Zone: rate of bacterial and phytoplankton growth and grazing by heterotrophic protists. Deep-Sea Res. Part II 58, 2248–2259.

Putt, M., Stoecker, D.K., 1989. An experimentally determined carbon:volume ratio for marine "oligotrichous" ciliates from estuarine and coastal waters. Limnol. Oceanogr. 34, 1097–1103.

Rintoul, S.R., Sokolov, S., 2001. Baroclinic transport variability of the Antarctic Circumpolar Current south of Australia (WOCE repeat section SR3). J. Geophys. Res. 106 (C2), 2815–2832.

Safi, K.A., Griffiths, F.B., Hall, J.A., 2007. Microzooplankton composition, biomass and grazing rates along the WOCE SR3 line between Tasmania and Antarctica. Deep-Sea Res. Part I 54, 1025–1041.

Selph, K.E., Landry, M.R., Allen, C.B., Calbet, A., Christiansen, S., Bidigare, R.R., 2001. Microbial community composition and growth dynamics in the Antarctic Polar Front and seasonal ice zone during late spring 1997. Deep-Sea Res. Part II 48, 4059–4080.

Sieburth, J.M., Smetacek, V., Lenz, J., 1978. Pelagic ecosystem structure: heterotrophic compartments of the plankton and their relationship to plankton size fractions. Limnol. Oceanogr. 23, 1256–1263.

Strom, S.L., Macri, E.L., Olsen, M., 2007. Microzooplankton grazing in the coastal Gulf of Alaska: variations in top-down control of phytoplankton. Limnol. Oceanogr. 52, 1480–1494.

Strickland, J.D.H., Parsons, T.R., 1972. A Practical Handbook of Seawater Analysis, Bulletin, second ed. : Fish. Res. Bull. Can. Canada, 167, p. 310.

Tréguer, P., Jacques, G., 1992. Dynamics of nutrients and phytoplankton, and fluxes of carbon, nitrogen, and silicon in the Antarctic Ocean. Polar Biol. 12, 149–162.

Tsuda, A., Kawaguchi, S., 1997. Microzooplankton grazing in the surface water of Southern Ocean during an austral summer. Polar Biol. 18, 240–245.

Verity, P.G., Langdon, C., 1984. Relationships between lorica volume, carbon, nitrogen and ATP content of tintinnids in Narragansett Bay. J. Plankton Res. 6, 859–868.

Verity, P.G., Stocker, D.K., Sieracki, M.E., Nelson, J.R., 1993. Grazing, growth and mortality of microzooplankton during the 1989 North Atlantic spring bloom at 471N 181W. Deep-Sea Res. Part II 40, 1793–1814.
Ward, P., Grant, S., Brandon, M., Siegel, V., Sushin, V., Loeb, V., Griffiths, H., 2004. Mesozooplankton community structure in the Scotia Sea during the CCAMLR 2000 Survey: January–February 2000. Deep-Sea Res. Part II 51, 1351–1367.
Ward, P., Shreeve, R., Atkinson, A., Korb, B., Whitehouse, M., Thorpe, S., Pond, D., Cunningham, N., 2006. Plankton community structure and variability in the Scotia Sea: austral summer 2003. Mar. Ecol. Prog. Ser. 309, 75–91.
Ward, P., Whitehouse, M., Meredith, M., Murphy, E., Shreeve, R., Korb, R., Watkins, J., Thorpe, S., Woodd-Walker, R., Brierley, A., Cunningham, N., Grant, S., Bone, D., 2002. The Southern Antarctic Circumpolar current: physical and biological coupling at South Georgia. Deep-Sea Res. Part I 49, 2183–2202.
Wylie, J.L., Currie, D.J., 1991. The relative importance of bacteria and algae as food source for crustacean zooplankton. Limnol. Oceanogr. 36, 708–728.